Anno 2010_Numero 158

rapporti tecnici INGV

Determination of the temperature field due to frictional heating on a sliding interface

158

Istituto Nazionale di Geofisica e Vulcanologia

Anno 2010_Numero 158

rapporti tecnici INGV

DETERMINATION OF THE TEMPERATURE FIELD DUE TO FRICTIONAL HEATING ON A SLIDING INTERFACE

Andrea Bizzarri

INGV (Istituto Nazionale di Geofisica e Vulcanologia, Sezione di Bologna)

158

Table of contents

Introduction

In the recent years we assisted to an increasing number of studies devoted to the quantification of the effects of temperature developed as a consequence of frictional heat on a sliding interface. The temperature field generated on the fault surface is responsible of a large number of physical and chemical dissipative process, summarized in Bizzarri (2010a).

Among these we mention here the flash heating of micro–asperity contacts, basically consisting in a different behavior of fault friction at high fault slip velocities [e.g., Bizzarri, 2009a; Noda et al., 2009], the melting of rocks and gouge particles [Nielsen et al., 2008; Bizzarri, 2010b], the thermally–induced pressurization of fluids in saturated fault structures [Andrews, 2002; Bizzarri and Cocco, 2006; Rice, 2006].

A key issue of all these studies is the proper calculation of the temperature distribution on the fault surface and its temporal evolution.

In this study we compare two different analytical solutions proposed in the literature with the special aim to clarify their prominent features, the numerical advantages and the different physical implications of each of them. In particular, we will compare the temporal evolution of the obtained temperature in the case of spontaneously spreading, fully dynamic rupture on a fault of finite width and we will show how the solutions can be reconciled.

1. The fault geometry

The fault geometry considered in this study is the same as that introduced in Bizzarri (2009b), briefly summarized here for completeness. As illustrated in Figure 1, the vertical, planar fault has dimensions L^f and W^f in the strike and dip directions, respectively. The fault is embedded in a surrounding elastic medium, discretized by mean of specialized parallelepids, having faces parallel to the Cartesian axes, x_1, x_2 and x_3.

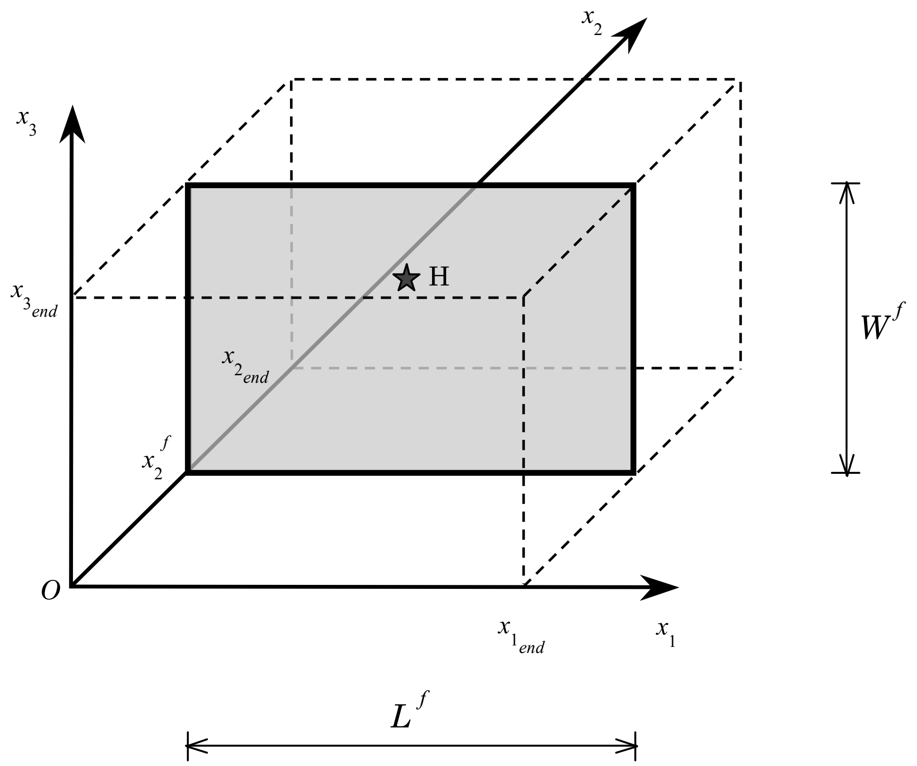

Figure 1. Schematic representation of the fault model considered in the present study. The grey plane $x_2 = x_2^f$ represents the fault, the star H indicates the hypocenter. Dashed lines denote the spatial extension of computational domain, $\Omega^{(FD)}$, having dimension $x1_{end}$, $x2_{end}$ and $x3_{end}$ in each direction. The plane $x_3 = 0$ is the free surface.

The plane $x_2 = x_2^f$ is governed by a fault constitutive law, the details of which are behind the goals of the present study. We simply mention here that the constitutive equation makes possible to (numerically) obtain the solution of the fundamental elasto–dynamic equation in the presence of medium discontinuity (the fault plane), where a spontaneous, dynamic rupture nucleates and further propagates.

In the remainder of the work we will denote with v the magnitude of the fault slip velocity and with τ the magnitude of the fault traction. Both the two variables (which are the solution of the spontaneous dynamic rupture problem) explicitly depend on the two on–fault coordinates x_1 and x_3 and on time t (so that the problem is 3–D). For sake of simplicity we consider a vertical strike slip fault, as in Figure 1.

2. The solution of Kato (2001)

Kato (2001) studies the evolution of a fault in its pre–seismic phase (i.e., that preceding the dynamic rupture propagation leading to stress release and seismic waves excitation in the medium surrounding the seismogenic structure), by using a simple 1–D spring–slider analog fault system. The novelty of that paper is the use of a modification of the classical analytical expression of the rate– and state–dependent constitutive relation [see Ruina, 1983 and references cited therein], accounting for an additional dependence on temperature developed on the frictional interface (the "fault" plane), as a consequence of the sliding of the mass block (i.e., frictional heat). In a generic point (x_1,x_3) of the plane $x_2 = x_2^f$, at a distance ζ from $x_2 = x_2^f$ along the off–fault direction (i.e., along the x_2 axis; see Figure 1) and at time t the temperature evolution due to a fault slip velocity history $v(t)$ and a traction history $\tau(t)$ is calculated by Kato (2001) following the solution of McKenzie and Brune (1972), which reads:

$$T(t) = T_0 + \frac{1}{2c\sqrt{\pi\chi}} \int_0^t \mathrm{d}t' \frac{e^{-\frac{\zeta^2}{4\chi(t-t')}}}{\sqrt{t-t'}} v(t')\tau(t') \tag{1}$$

where T_0 is the initial temperature (i.e., at $t = 0$) and c is the heat capacity of the bulk composite for unit volume, χ is the thermal diffusivity. In equation (1) v and τ are calculated in the point (x_1,x_3) of the plane $x_2 = x_2$, where also T is calculated. In other words, (x_1,x_3) is the normal projection on the fault of the point where T is computed.

If we consider the limit of $t' \to t$, we have that the integrand in equation (1) vanishes, so we can safely rewrite previous equation as

$$T(t) = T_0 + \frac{1}{2c\sqrt{\pi\chi}} \int_0^{t-\varepsilon} \mathrm{d}t' \frac{e^{-\frac{\zeta^2}{4\chi(t-t')}}}{\sqrt{t-t'}} v(t')\tau(t') \tag{2}$$

where ε is an arbitrarily small, positive, real number. Moreover, in the limit of $\zeta \to 0$ (which physically identifies the fault plane) equation (2) can be further simplified:

$$T(t) = T_0 + \frac{1}{2c\sqrt{\pi\chi}} \int_0^{t-\varepsilon} \mathrm{d}t' \frac{1}{\sqrt{t-t'}} v(t')\tau(t') \tag{3}$$

Equation (3) can be calculated numerically as follows:

$$T^m = \begin{cases} T_0 & , m = 1 \\ T_0 + \dfrac{1}{2c\sqrt{\pi\chi}} \displaystyle\sum_{n=1}^{m-1} \dfrac{1}{\sqrt{(m-n)\Delta t}} v^n \tau^n \Delta t & , m > 1 \end{cases} \tag{4}$$

in which the apex (m or n) denotes the time level at which the variables are evaluated and Δt is the time discretization (leading to $t^m = m\Delta t$). We note that the quantity ε in equation (3) is represented by Δt in equation (4); this is numerically correct, provided that the time step Δt is sufficiently small (see section 4). Indeed, the requirement that Δt is sufficiently small is necessary also for a proper resolution of the elasto–dynamic problem, as discussed in details in Bizzarri and Cocco (2005).

We have demonstrated that equation (4) is numerically equivalent to the equation (12) proposed by Kato (2001) to discretize equation (3), reported here for completeness:

$$T^m = T_0 + \frac{1}{c\sqrt{\pi\chi}} \sum_{n=1}^{m} \left(\sqrt{(m-n+1)\Delta t} - \sqrt{(m-n)\Delta t}\right) v^{n-1} \tau^{n-1} \tag{5}$$

with $v^0 = \tau^0 = 0$.

3. The solution of Bizzarri and Cocco (2006)

Geological evidences [Chester and Chester, 1998; Billi and Storti, 2004] suggest that a seismogenic fault is composed by an inner fault core, where the principal slipping zone is located and where the slip is concentrated, surrounded by a fractured damage zone, located before the undamaged host rock. By assuming this kind of fault model [see also Sibson, 2003], Bizzarri and Cocco (2006) consider the frictional heat due to a heat source

$$q(\zeta, t) = \begin{cases} \dfrac{\tau(t) v(t)}{2w} & , t > 0, |\zeta| \le w \\ 0 & , |\zeta| > w \end{cases} \tag{6}$$

where $2w$ is the thickness of the slipping zone. The Fourier's equation

$$\frac{\partial}{\partial t} T(\zeta, t) = \chi \frac{\partial^2}{\partial \zeta^2} T(\zeta, t) + \frac{1}{c} q(\zeta, t) \tag{7}$$

again in the limit $\zeta \to 0$, has then the following solution:

$$T(t) = T_0 + \frac{1}{2cw} \int_0^{t-\varepsilon} \mathrm{d}t' \, \mathrm{erf}\left(\frac{w}{2\sqrt{\chi (t - t')}} \right) v(t') \tau(t') \tag{8}$$

in which the erf(.) is the error function ($\mathrm{erf}(z) \underset{\mathrm{df}}{=} \frac{2}{\sqrt{\pi}} \int_0^z \mathrm{d}x \, \mathrm{e}^{-x^2}$). The numerical counterpart of equation (8) reads:

$$T^m = \begin{cases} T_0 & , m = 1 \\ T_0 + \dfrac{1}{2cw} \displaystyle\sum_{n=1}^{m-1} \mathrm{erf}\left(\frac{w}{2\sqrt{\chi (m - n) \Delta t}} \right) v^n \tau^n \Delta t & , m > 1 \end{cases} \tag{9}$$

where m or n denote the time level, as in equations (4) and (5).

4. Comparison of the different solutions

In this section we will compare the temperature evolution obtained by Kato (2001; see previous equation (5)) and that obtained by Bizzarri and Cocco (2006; see previous equation (9)).

A first important feature we want to emphasize is that both the solutions exhibit a de–coupling between temperature evolution and the histories of fault slip velocity and traction. In other words, the temperature field computed at time level m depends on the time evolution of v and τ, up to the time level $m - 1$ (i.e., the previous one). From a computational point of view this means that the calculation of T at time level m is straightforward, in that we already know all the needed quantities from previous numerical iterations.

In order to compare the two solutions (equations (5) and (9)) we will consider a typical evolution of fault slip velocity and traction, obtained in a dynamic rupture simulation. These solutions have been obtained numerically, via the finite difference code described in detail in Bizzarri and Cocco (2005). On the considered strike slip vertical fault we select a receiver located at the hypocentral depth and at a distance from the hypocenter along the strike direction such that the time histories are not influenced neither by the nucleation nor by the presence of the fault boundaries (the fault has finite extension). The behavior of v and τ for that receiver is reported in Figure 2.

The specific details about these solutions are behind the main purposes of the present work; we can simply keep them as sufficiently representative of a typical crustal earthquake. They have been obtained by using a very fine temporal discretization ($\Delta t = 6.94 \times 10^{-4}$ s), so that the quantity ε in equations (3) and (8) makes the numerical approximations (5) and (9) reliable.

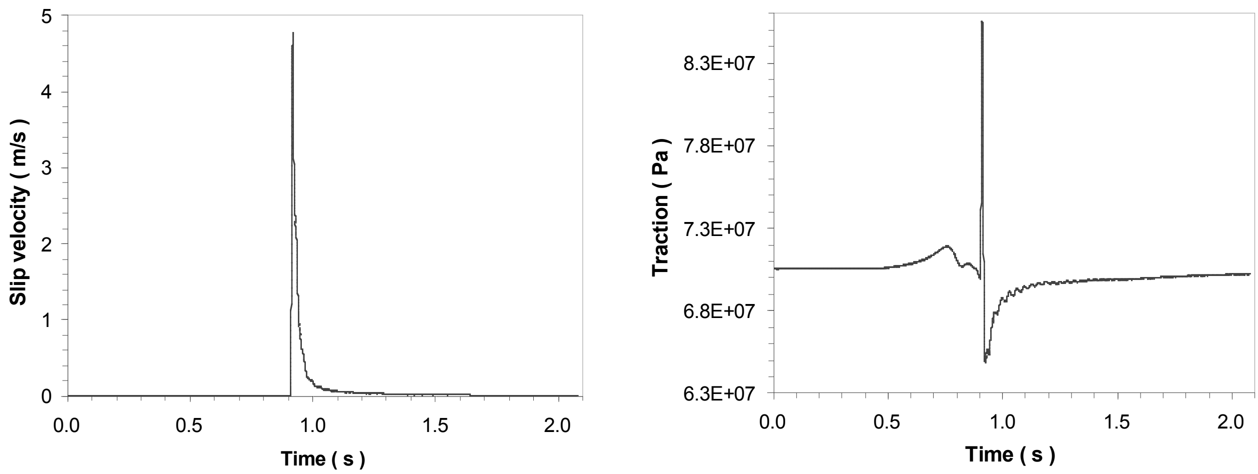

(a) **(b)**

Figure 2. Time evolutions of the fault slip velocity (panel (a)) and traction (panel (b)) considered for the comparison between the two solutions for the temperature field. The solutions pertain to a fault receiver located at hypocentral depth and sufficiently far from the hypocenter and from the fault boundaries.

By using the time histories $\{v^m\}$ and $\{\tau^m\}$ reported in Figure 2 we compute the temperatures as obtained from equations (5) and (9). The results are displayed in Figure 3.

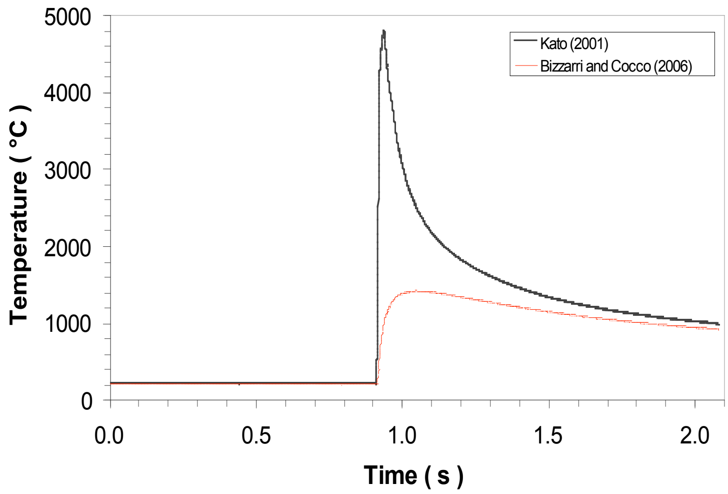

Figure 3. Comparison between the two solutions for the temperature evolution for the time histories reported in Figure 2.

From Figure 3 we can clearly see that for a typical value of the slipping zone thickness (w = 1 mm) the two solutions are rather different. We can see that the final value of T is nearly the same (the two curves asymptotically reach the same final value). However, the behavior during the accelerating phase (when the fault slip velocity increases up the its maximum value) and also during the stress release (when the traction degrades from upper yield stress down to the kinetic level) is markedly different in the two cases.

Notably, the temperature predicted by the solution of Kato (2001) (black line in Figure 3) exceeded the melting temperature (which in turn would cause a state change in the gouge material and rocks, from their solid state to the molten state). Moreover, the temperatures predicted by equation (5) appear to be excessively high and basically unrealistic. On the contrary, the time evolution of the temperature predicted by equation (9) (red curve in Figure 3) would remain below the melting point.

5. How to reconcile the solutions

It is evident from Figure 3 that the predictions of the temperature evolution on the fault given by equations (5) and (9) are rather different. In this section we will show that the two solutions can be reconciled, under proper assumptions.

Bizzarri and Cocco (2006) have extensively explored the behavior of a propagating 3–D earthquake rupture and the consequent developed temperature as a function of the parameters of the model. Indeed, it has been clearly demonstrated that the key parameter controlling the temperature evolution is the thickness of the slipping zone ($2w$), as physically expected.

In Figure 4 we compare the time histories of T obtained by considering different values of w, by varying this parameter within the range suggested by laboratory inferences and geological observations. In Figure 4 the thick, black curves is still the solution by Kato (2001).

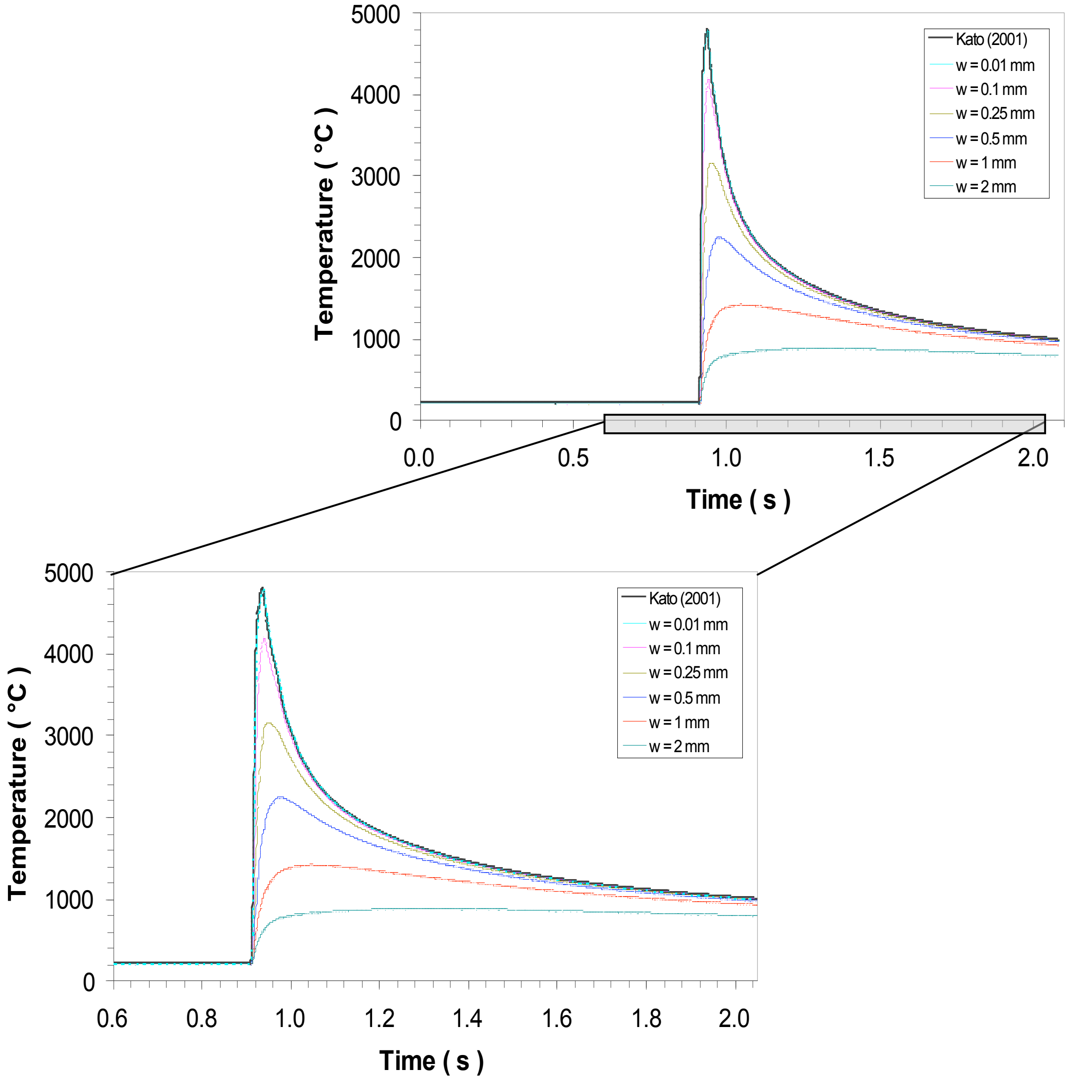

Figure 4. Effects of the different values of the thickness of the slipping zone (values are reported in the legends). Thick, black curves reports the solution by Kato (2001) for a better comparison. Bottom panel display a zoom in the time window marked on the top panel.

As expected, we can see from Figure 4 that by increasing the value of w the developed temperature progressively decreases. This is physically reasonable, in that large values of w imply that the heat input $v\tau$ is distributed over a larger spatial extension in the off–fault direction.

Interestingly, we can note that for w = 10 μm the solution by Kato (2001) and by Bizzarri and Cocco (2006) are substantially identical, in that the two curves are indistinguishable. We have also proven that for $w \leq$ 10 μm the temperatures predicted by equation (9) are unchanged with respect to that pertaining to the case of w = 10 μm.

6. Summary

The sliding on an interface generates frictional heating, finally leading to a variations in the temperature field. Indeed, the calculation of the temperature change is extremely important in the dynamic modeling of the seismic source, since there is a large number of thermally–activated chemico–physical phenomena occurring during an earthquake rupture and influencing its dynamic propagation on that interface [see Bizzarri, 2010a for a review].

In this study we have compared two analytically and conceptually different solutions for the temperature field generated during an earthquake rupture. The first one has been proposed by Kato (2001) on the basis on the “classical” (or traditional) models of heat conduction, relying on the framework of McKenzie and Brune (1972). The second one has been derived by Bizzarri and Cocco (2006), on the basis of a more realistic seismogenic model, corroborated by some geological evidence, in which the heat source is distributed over a slipping zone, having a finite width.

Through numerical calculations we have demonstrated here that, during a cosesimic rupture where the values of the fault slip velocity are of the order of several meters per second, the two solutions are rather different.

In particular, the prediction of Kato (2001) would lead to extremely high temperatures, greater that the melting point and unrealistic (without the account of a state change, the developed temperature change would reach values comparable with those attributed to the Earth’s core).

In this study we have also shown that for values of the slipping zone half–thickness (w) smaller that 10 μm the two solutions can be reconciled, since they are substantially equivalent. We want to emphasize that holds (k being a constant):

$$\lim_{w \to 0^+} \frac{\operatorname{erf}\left(\frac{w}{k}\right)}{w} = \frac{2}{\sqrt{\pi}\, k} \tag{10}$$

If we consider the limit for $w \to 0^+$ of equation (9), considering the result in equation (10), with $k = 2\sqrt{\chi(m-n)\Delta t}$, we obtain exactly equation (4), that we recall is numerically identical to the solution of Kato (2001; our equation (12)). For typical thermal parameters and for typical velocity and traction histories we have proven that w = 10 μm makes the two solutions substantially equivalent.

To conclude, the solution of Kato (2001) can be considered as a simplified version of the more general solution found by Bizzarri and Cocco (2006). It can be eventually employed to compute the temperature evolution during the interseismic phase, when sliding velocities are very small and the consequent temperature change is not so important as during the cosesimic time window. Moreover, the solution by Kato (2001) can be used in dynamic models of cosesimic ruptures only in cases when the slip is extremely localized (so that w = 10 μm of less).

References

Andrews, D. J. (2002). A fault constitutive relation accounting for thermal pressurization of pore fluid, J. Geophys. Res., 107, No. B12, 2363, doi: 10.1029/2002JB001942.

Billi, A., Storti, F. (2004). Fractal distribution of particle size in carbonate cataclastic rocks from the core of a regional strike–slip fault zone, Tectonophys., 384, 115–128.

Bizzarri, A. (2009a). Can flash heating of asperity contacts prevent melting?. Geophys. Res. Lett., 36, L11304, doi: 10.1029/2009GL037335

Bizzarri, A. (2009b). On the implementation of Absorbing Boundary Conditions in a Finite Difference code with conventional grid, Rapporti Tecnici I.N.G.V., 122, 1 – 18

Bizzarri, A. (2010a). Toward the formulation of a realistic fault governing law in dynamic models of earthquake ruptures, in *Dynamic Modelling*, Edited by Alisson V. Brito, INTECH, Vienna, ISBN 978-953-7619-68-8, 167–188, http://www.sciyo.com/articles/show/title/toward-the-formulation-of-a-realistic-fault-governing-law-in-dynamic-models-of-earthquake-ruptures

Bizzarri, A. (2010b). An efficient mechanism to avert frictional melts during seismic ruptures, Earth Plan. Sci. Lett., 296, Nos. 1–2, 144 – 152, doi: 10.1016/j.epsl.2010.05.012

Bizzarri, A., Cocco, M. (2005). 3D dynamic simulations of spontaneous rupture propagation governed by different constitutive laws with rake rotation allowed. Ann. Geophysics, 48, No. 2, 279–299

Bizzarri, A., Cocco, M. (2006). A thermal pressurization model for the spontaneous dynamic rupture propagation on a three–dimensional fault: 1. Methodological approach, J. Geophys. Res., 111, B05303, doi: 10.1029/2005JB003862.

Chester, F. M., Chester, J. S. (1998). Ultracataclasite structure and friction processes of the Punchbowl fault, San Andreas system, California, Tectonophys., 295, 199–221.

Kato, N. (2001). Effect of frictional heating on pre–seismic sliding: a numerical simulation using a rate–, state– and temperature–dependent friction law, Geophys. J. Int., 147, 183–188

McKenzie, D., Brune, J. N. (1972). Melting on fault planes during large earthquakes, Geophys. J. R. astr. Soc., 29, 65–78.

Nielsen, S., Di Toro, G., Hirose, T., Shimamoto, T. (2008). Frictional melt and seismic slip, J. Geophys. Res., 113, B01308, doi: 10.1029/2007JB005122.

Noda, H., Dunham, E. M., Rice, J. R. (2009). Earthquake ruptures with thermal weakening and the operation of major faults at low overall stress levels, J. Geophys. Res., 114, B07302, doi: 10.1029/2008JB006143.

Rice, J. R. (2006). Heating and weakening of faults during earthquake slip, J. Geophys. Res., 111, B05311, doi: 10.1029/2005JB004006.

Ruina, A. L. (1983). Slip instability and state variable friction laws, J. Geophys. Res., 88, 10,359–10,370.

Sibson, R. H. (2003). Thickness of the seismic slip zone, Bull. Seism. Soc. Am., 93, No. 3, 1169–1178.

Coordinamento editoriale e impaginazione
Centro Editoriale Nazionale | INGV

Progetto grafico e redazionale
Laboratorio Grafica e Immagini | INGV Roma

Via di Vigna Murata, 605
00143 Roma
Tel. +39 06518601 Fax +39 065041181

http://www.ingv.it

Istituto Nazionale di Geofisica e Vulcanologia